Journal of Solid State Chemistry **146**, 6–12 (1999)
Article ID jssc.1999.8258, available online at http://www.idealibrary.com on IDEAL®

Effect of Homovalent Anion Doping on the Conductivity and Phase Transitions in Na_2SO_4

S. Gomathy, P. Gopalan,[1] and A. R. Kulkarni

Department of Metallurgical Engineering and Materials Science, Indian Institute of Technology, Bombay 400 076, India

Received September 11, 1998; in revised form February 23, 1999; accepted March 10, 1999

An attempt has been made to understand the effect of doping homovalent anion dopants such as CO_3^{2-}, $B_4O_7^{2-}$, MoO_4^{2-}, and WO_4^{2-} on the conductivity and phase transitions of Na_2SO_4 by means of XRD, DSC, and impedance measurements. Our studies indicate that the observed conductivity enhancement is largely due to an increase in the free volume in the structure. Apart from the size, the shape and orientational ordering of the dopant ion in the sulfate sublattice seem to influence the activation energy. The structure of the guest anion appears to be one of the major factors determining the phase stabilization of Na_2SO_4 (I) at low temperatures. © 1999 Academic Press

1. INTRODUCTION

Sodium sulfate exhibits five polymorphs. The various transformations occur in the following manner (1).

$$V \leftrightarrow (IV) \overset{200^\circ C}{\leftrightarrow} III \overset{228^\circ C}{\leftrightarrow} II \overset{235^\circ C}{\leftrightarrow} I \overset{883^\circ C}{\leftrightarrow} \text{Melt}$$

The high-temperature phase (I) has a hexagonal structure with space group, $P6_3/mmc$, and is characterized by orientational disorder of the SO_4 tetrahedra in the sulfate sublattice (2). The first-order transition at 235°C is due to the transition from rotation to oscillation of the SO_4 ions and is accompanied by a slight change in crystal symmetry. Consequently, all the low-temperature phases have orthorhombic pseudo-hexagonal structures with slightly differing space groups.

The III↔I phase transition at 241°C (3) is accompanied by a large increase in the c/a axial ratio that results in a volume expansion of about 4% and is assumed to be responsible for the observed order of magnitude increase in Na ion conductivity in the high-temperature phase (4). The direct correlation between structural change and conductivity increase suggests a percolation-type ion transport mechanism in Na_2SO_4, wherein an increase in the number of intersite channel connectivities at the phase transition temperature increases the freedom of cation movement and, thereby, an enhancement in Na ion conductivity.

The main limitations of Na_2SO_4 as a solid electrolyte in SO_x gas sensors are its low conductivity and the volume changes accompanying the phase transitions, leading to microcracks in the material (5–7). Fortunately, sodium sulfate forms extensive solid solutions with other sulfates (3, 8) and has, therefore, thrown open a very broad range of systems that could be examined to enhance the conductivity and suppress the phase transitions.

The ionic conductivity of Na_2SO_4 (I) can be increased by almost 2–3 orders of magnitude by the addition of aliovalent dopants (9–18). The conductivity enhancement in such systems is strongly correlated to the increase in vacancy concentration. However, the effect of size mismatch between the guest and host ions on the Na ion conductivity has only been resolved recently (17). Secco and co-workers (4, 10, 18) have carried out extensive research on the effect of homovalent doping on the ionic conductivity of Na_2SO_4 (I). Their studies on the homovalent doping of Na_2SO_4 indicate an appreciable increase in conductivity in the presence of larger radius ions such as Rb^+, Ag^+, MoO_4^{2-}, and WO_4^{2-}. The increase in conductivity is largely attributed to simple lattice expansion, effected by the incorporation of larger guest ions. While in the case of the Ag^+ doped system the high ionic conductivity is attributed to the presence of the highly mobile Ag^+ species, the effect of doping larger size ions such as K^+ (4) and SeO_4^{2-} (19) has been only a small increase in conductivity. An enhancement in Na^+ conductivity with the addition of the smaller Li^+ dopant has also been reported (10, 20). The investigations of Na_2SO_4 clearly point to a complex relationship between the structure and the conductivity of the system. A thorough investigation of homovalently doped systems will provide more insight on the role of the wrong size dopant.

In the present investigation, we have made a systematic study of the effect of homovalent anion doping on sodium sulfate. By choosing homovalent anion dopants, this investigation focuses on factors other than charge

[1] To whom correspondence should be addressed.

0022-4596/99 $30.00

carrier concentration; for example, ion size, cation–anion interactions, etc. that influence the conductivity and phase transitions inherent to the system have been investigated. The anions chosen for the present study include CO_3^{2-}, $B_4O_7^{2-}$, MoO_4^{2-}, and WO_4^{2-}.

2. EXPERIMENTAL PROCEDURE

Three different compositions of each dopant, namely, 2, 5, and 10 mol% (m/o) dopant concentration, were investigated. An additional composition was studied in the Na_2CO_3 doped system. The starting materials used were anhydrous Na_2SO_4, anhydrous Na_2CO_3, and $Na_2B_4O_7 \cdot 10H_2O$ procured from Loba Chemie, Bombay, and $Na_2MoO_4 \cdot 2H_2O$ and $Na_2WO_4 \cdot 2H_2O$ procured from Aldrich Chemicals, USA. Ultrapure Na_2SO_4, obtained from Aldrich Chemicals, USA, was used for measurements on the undoped samples. The powders were carefully weighed in appropriate molar quantities, ground, and then melted in porcelain crucibles. The melted samples were then quenched and powdered. For conductivity measurements, the powders were pressed into pellets (5 tons/cm^2). All the pellets were 2–4 mm in thickness and 10 mm in diameter. Gold was sputtered on the two flat surfaces of the pellet to ensure good electrical contact with the platinum electrodes of a sample holder.

The ac impedance was measured in air during the cooling cycle at frequencies ranging between 1 and 32 MHz using a Solartron Impedance Analyzer, Model Schlumberger SI1260. From the complex impedance plots thus generated, dc conductivity was extracted. The DSC measurements were made with a DSC V2.2A DuPont 9900 calorimeter. XRD patterns were recorded using Cu$K\alpha$ radiation with the help of a PW1820 Philips diffractometer.

3. RESULTS AND DISCUSSIONS

3.1. XRD

Analysis of the room-temperature X-ray diffraction patterns of the compositions studied in the binary systems indicate the presence of either Na_2SO_4 (III) or Na_2SO_4 (V) or both. Table 1 summarizes the XRD results of the present study.

Traces of phase I could be identified at room temperature in the 2 mol% Na_2CO_3 doped composition. However there is no evidence of this phase in the compositions containing 5 and 10 mol% Na_2CO_3. Instead a new phase, $2Na_2SO_4 \cdot Na_2CO_3$, is observed in the 10 mol% composition. To determine the extent to which Na_2CO_3 is effective in quenching phase I at room temperature, another intermediate composition (4 mol%) was prepared and characterized. The XRD pattern of this composition also contained lines corresponding to phases I, III, and V. These results are more or less in agreement with an earlier report that phase I can be stabilized in solid solutions containing up to 5 mol% Na_2CO_3 (21).

TABLE 1
Phases Observed in the Room-Temperature XRD of the Doped Na_2SO_4 Systems

	Phases observed in room-temperature XRD for varying concentrations of dopants		
Binary system	2 mol%	5 mol%	10 mol%
Na_2SO_4–Na_2CO_3	Na_2SO_4 (V, III, I)	Na_2SO_4 (III)	Na_2SO_4 (V, III) $2Na_2SO_4 \cdot Na_2CO_3$
Na_2SO_4–$Na_2B_4O_7$	Na_2SO_4 (III)	Na_2SO_4 (V)	Na_2SO_4 (III)
Na_2SO_4–Na_2MoO_4	Na_2SO_4 (III, I)	Na_2SO_4 (V, III, I)	Na_2SO_4 (V, I)
Na_2SO_4–Na_2WO_4	Na_2SO_4 (V, III, I)	Na_2SO_4 (V, III) $Na_2WO_4 \cdot 2H_2O$	Na_2SO_4 (V, III) $Na_2WO_4 \cdot 2H_2O$

In the sodium borate doped compositions, a systematic negative shift in the *d*-line spacing (compared to those of pure Na_2SO_4 III and V) is observed, the shift being most pronounced in the 10 mol% composition. This lattice contraction is most likely indicative of the presence of smaller size borate ions.

Most of the intermediate and weak lines of the molybdate doped samples match with those of phase I. With increasing concentration of Na_2MoO_4, the number of lines corresponding to this phase decreases. In the 10 mol% composition, a few lines of intermediate and weak intensity could not be matched with any known phase. Chen *et al.* (22) have reported the formation of a new phase, $Na_2Mo_{0.1}S_{0.9}O_4$, in the composition containing 10 mol% Na_2MoO_4. In the absence of the powder diffraction data, it was not possible to verify the presence of this phase in our samples.

In the tungstate doped compositions, phase I is present only in the 2 mol% doped composition. Because none of the polymorphs of Na_2WO_4 are isomorphous with Na_2SO_4 (I), it has lower solid solubility in Na_2SO_4 compared to Na_2MoO_4. The presence of Na_2WO_4 in the 5 and 10 mol% compositions indeed confirms the low solid solubility limit of sodium tungstate in Na_2SO_4.

3.2. DSC

Figure 1 shows the DSC curves of the 2 mol% doped compositions. The peaks occurring between 220 and 250°C in all the compositions may be related to the V → III and/or III → I phase transitions in Na_2SO_4.

The presence of 5 and 10 mol% anion dopants in Na_2SO_4 does not seem to have any significant effect on the III → I phase transition temperature of Na_2SO_4, except for lowering it by ~10–20°C. An additional peak is observed at ~450°C in the 5 mol% molybdate doped system. This may be attributed to the IV → III transition that occurs at 444°C in pure Na_2MoO_4 (23). The peaks occurring at 255 and

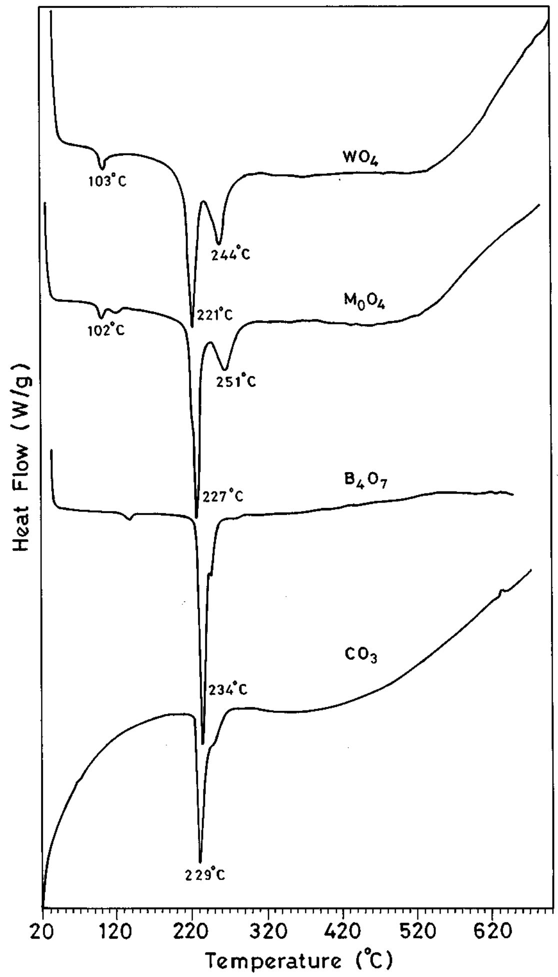

FIG. 1. DSC traces of Na_2SO_4 systems for 2 mol% concentration of various anion dopants.

438°C in the 10 mol% Na_2MoO_4 composition appear to be those corresponding to the phase transitions in $Na_2Mo_{0.1}S_{0.9}O_4$ (22). High-temperature peaks are also observed at $\sim$250 and 640°C in the 5 and 10 mol% Na_2WO_4 doped compositions. These may once again be related to the phase transitions occurring in Na_2WO_4 (23). Surprisingly, the phase diagram of this binary indicates complete solid solutions in the Na_2SO_4-rich regions at these temperatures (24).

3.3. Conductivity

Pure Na_2SO_4. The ionic conductivity of Na_2SO_4 obeys the Arrhenius-type behavior for conduction in ionic solids and is given by

$$\sigma T = \frac{nq^2\lambda^2 v}{k}\exp(-Q_c/RT) = \sigma_0 \exp(-Q_c/RT) \quad [1]$$

In this expression, n is the number of activated charge carriers per unit volume, λ is the distance between neighboring Na ions, v is the lattice vibrational frequency, R is the universal gas constant, and k is the Boltzmann constant. The activation energy Q_c is a composite quantity involving the activation energies of formation and migration of defects. Na_2SO_4 is expected to exhibit cationic Frenkel defects due to the smaller size of the sodium ions compared to that of the sulfate ions (9). Since the sodium interstitials are more mobile than the sodium vacancies (12), the contribution to activation energy from the migration of vacancies is usually neglected. In the extrinsic region of conductivity, the enthalpy of formation of defects is negligible and the observed activation energy is taken as that required for migration of the Na interstitials.

In this study, the conductivity of pure Na_2SO_4 having different grades of purity (99.5 and 99.99%) was measured. The conductivity of the pure sample is found to be at least eight times higher than that of the ultrapure sample at all temperatures (Fig. 2). The conductivity dependence on sample purity clearly indicates that this is the extrinsic region of Na_2SO_4.

The conductivity jump for the ultrapure sample at $\sim$240°C is in agreement with the phase transition peak observed in DSC. The conductivity of the ultrapure sample is 2×10^{-6} $ohm^{-1}cm^{-1}$ at 300°C and is comparable to the values reported in literature (5, 25). The activation energy of the ultrapure sample is $\sim$51 kJ/mol between 240 and 450°C. This is also in complete agreement with the reported values of 50 ± 5 kJ/mol (9, 10, 26). Using Eq. [1], our high-temperature data yields the following conductivity equation

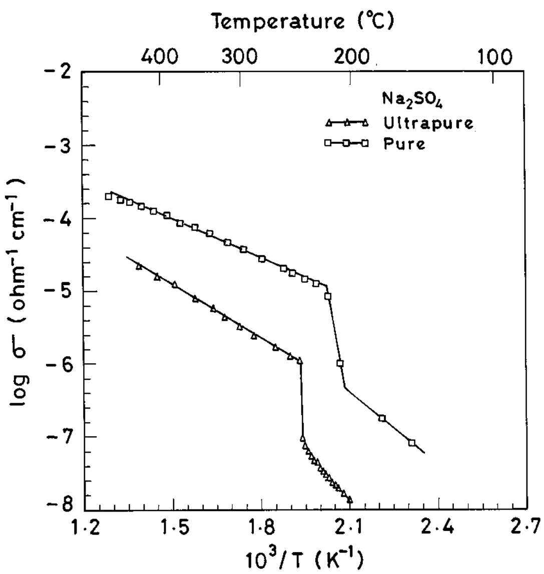

FIG. 2. Logσ vs $10^3/T$ plots of pure (99.5% purity) and ultrapure (99.99% purity) Na_2SO_4.

for the ultrapure sample:

$$\sigma T = 76.2\exp(-51000/RT)\,\mathrm{ohm}^{-1}\,\mathrm{cm}^{-1}\mathrm{K} \quad (240\text{–}450^\circ\mathrm{C}) \qquad [2]$$

Mixed anion systems. Figures 3 to 6 show the plots of $\log\sigma$ vs $10^3/T$ of the four Na_2SO_4-based mixed anion systems. The plots are fairly linear in the high-temperature region for all the compostions. Using the high-temperature conductivity data, the corresponding values of the activation energy, preexponential factor, conductivity, and conductivity enhancement ratio with regard to ultrapure sample are presented in Table 2. All the doped compositions show an enhancement in Na ion conductivity. For 2 mol% dopant composition, the tungstate ion doped composition shows the highest conductivity between 250 and 500°C, followed by the carbonate and molybdate ion doped compositions, and, finally, the tetraborate ion doped composition. For 5 mol% dopant concentration, the composition containing the molybdate ions has the highest conductivity between room temperature and 500°C, followed by those containing the tungstate, borate, and carbonate ions, respectively. The trend in conductivity for the compositions containing 10 mol% dopant concentration is similar to that of the 5 mol% doped systems at high temperatures (above 350°C). However, between 210 and 350°C, the borate ion doped composition has a higher conductivity than the tungstate doped composition.

Effect on Q_c. A comparison of the activation energies and preexponential factors of the pure and doped Na_2SO_4 systems reveals that the observed enhancement in Na ion conductivity is largely due to the decrease in the values of Q_c.

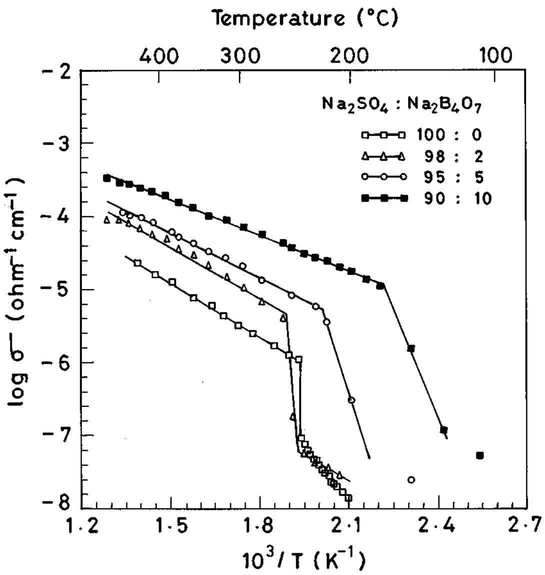

FIG. 4. $\log\sigma$ vs $10^3/T$ plots for three different compositions of the Na_2SO_4–$Na_2B_4O_7$ system.

A change in the activation energy of migration for the ions is generally expected whenever there is a size mismatch between the guest and host ions (11). When the host ions are substituted by ions of a smaller size, the lattice contracts and thereby hinders the motion of the host ions. Following the same reasoning, it is expected that lesser energy needs to be expended by an ion migrating through an expanded lattice.

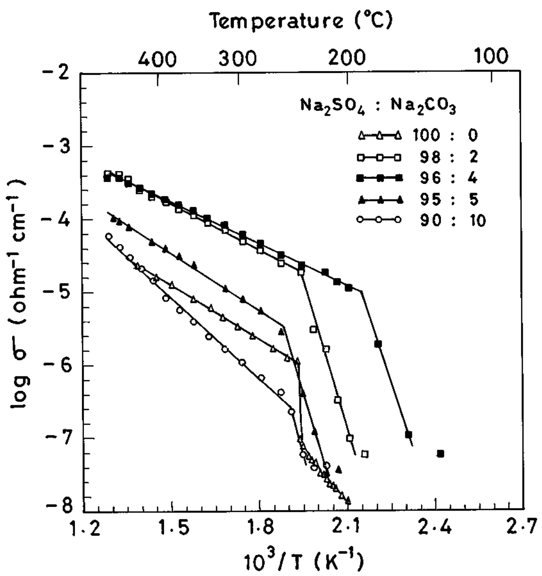

FIG. 3. $\log\sigma$ vs $10^3/T$ plots for four different compositions of the Na_2SO_4–Na_2CO_3 system.

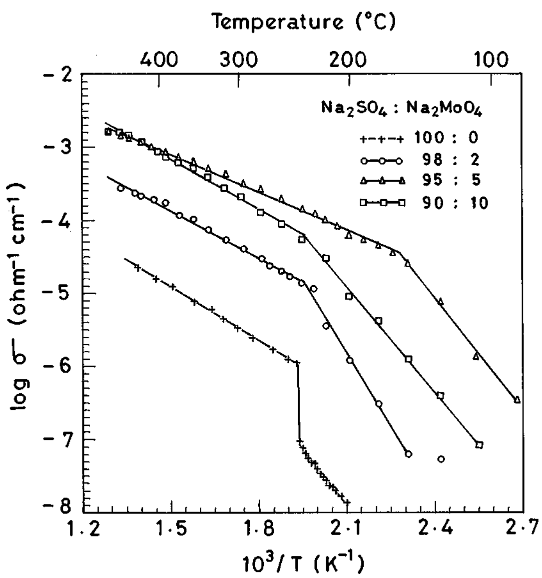

FIG. 5. $\log\sigma$ vs $10^3/T$ plots for three different compositions of the Na_2SO_4–Na_2MoO_4 system.

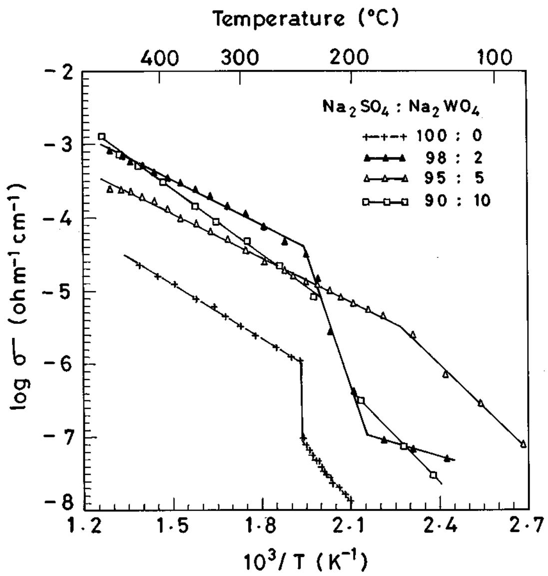

FIG. 6. Log σ vs $10^3/T$ plots for three different compositions of the Na_2SO_4–Na_2WO_4 system.

In the present study, the activation energies of migration are found to be lower than that of pure Na_2SO_4 in both the smaller and larger size ion doped compositions. The activation energy is lowered by a maximum of 34% in the 10 mol% B_4O_7 doped composition. At 2 mol% dopant concentration where all the dopants are completely soluble in Na_2SO_4, the compositions doped with the smallest anion, CO_3^{2-}, and the larger anion, MoO_4^{2-}, have comparable activation energies.

The relatively low activation energy of the carbonate ion doped system may be attributed to the shape and orientation of these ions in the sulfate lattice. According to Mehrotra *et al.* (27), the planar carbonate groups are oriented perpendicular to the *c* axis in Na_2SO_4 (I). The fact that the c/a ratio of Na_2SO_4 (I) and that of Na_2SO_4 (I) stabilized in solid solutions of Na_2CO_3 are comparable indicate that there is no change in the bottleneck size for the diffusing Na ions along directions parallel to the *a* and *b* axes. The activation energy, however, is found to decrease only to 4 mol% dopant concentration, suggesting that the orientational ordering of the carbonate ions is possible only to a limited extent. The stabilization of phase I in the 2 and 4 mol% doped compositions alone (as indicated by the respective XRD patterns) validates our point. At higher concentrations, the effect due to lattice contraction becomes predominant and increases the activation energy.

Similar to the case of the carbonate doped system, the activation energy decreases with increasing concentration of the borate ions. However, the B_4O_7 ion is considered to be larger than the CO_3 ion since the size of the BO_3 ion itself is 1.91 Å (28).

The activation energies of the Na_2MoO_4 and Na_2WO_4 doped systems are lower than the activation energy of the undoped system as expected since both the MoO_4 and WO_4 tetrahedra are larger than the sulfate ion. At low dopant concentrations (2 mol%), the larger size WO_4 dopant results in a lower activation energy. At higher dopant concentrations, the observed increase in activation energy can be attributed to the formation of an additional phase in the 10 mol% molybdate doped system. This also appears to be the case for the 5 and 10 mol% tungstate doped systems, as indicated by our XRD and DSC results. Our activation energy value for the 10 mol% Na_2MoO_4 doped system is

TABLE 2
Conductivity Results and Enhancement Factors for Various Anion Dopants

Dopant	Composition	Activation energy, Q_c (kJ/mol)	Temperature range (°C)	Preexponential exponential factor, σ_0	Conductivity, σ ($ohm^{-1}\,cm^{-1}$) at 395°C	σ/σ_{pure} at 395°C
Na_2CO_3	98:2	44.6	240–500	340	1.6×10^{-4}	14
	96:4	40.8	190–500	180	1.7×10^{-4}	15
	95:5	56.7	256–500	614	3.4×10^{-5}	3
	90:10	76.5	253–500	5322	8.3×10^{-6}	0.7
$Na_2B_4O_7$	98:2	50.3	258–500	233	4.1×10^{-5}	3
	95:5	43.3	222–500	102	6.3×10^{-5}	5
	90:10	33.8	180–500	52	1.8×10^{-4}	15
Na_2MoO_4	98:2	44.6	234–500	283	1.4×10^{-4}	18
	95:5	34.4	170–500	260	7.9×10^{-3}	67
	90:10	45.9	234–500	1793	6.9×10^{-3}	59
Na_2WO_4	98:2	38.2	239–500	200	3.1×10^{-4}	26
	95:5	40.8	170–500	121	1.2×10^{-4}	10
	90:10	56.1	227–500	3901	2.4×10^{-4}	20
Na_2SO_4	100:0	51	240–560	76.2	1.2×10^{-5}	1

found to be comparable with the reported value of 44 ± 3 kJ/mol (10). The high conductivity of the composition containing 10 mol% Na_2WO_4 may be due to a composite effect wherein the conductivity of a solid electrolyte phase is enhanced by dispersing phases of low ionic conductivity. This kind of behavior is more commonly observed in anion doped Li_2SO_4 binary systems due to the low solubility of the guest compounds in the latter (29, 30).

The high polarizability of the anion dopants is another factor that hampers the motion of the Na ions. These anions act as trap sites for the mobile ions and thereby increase the activation energy required for their migration. However, it is evident from the activation energies of the highly polarizable MoO_4 and WO_4 doped systems that the effect due to lattice expansion is more predominant.

Effect on σ_0. A marginal increase in σ_0 is observed in all the doped systems, with the exception of the 10 mol% B_4O_7 doped system. At 2 mol% dopant concentration, the composition containing the CO_3 dopant shows the highest enhancement in σ_0 (~6%) while the WO_4 ion shows the least enhancement (~2.5%).

The values of the jump distance (λ) and jump frequency (v) of the ions are not likely to change significantly, provided the type of mobile ion species and lattice structure remain the same in the doped systems. Hence it may be inferred that the addition of homovalent anion dopants slightly increases the number of activated sodium ions, n, in the Na_2SO_4 lattice. The increase in n may be explained on the basis of a *lattice loosening* effect wherein the lattice strain caused by the presence of wrong size dopants reduces the lattice binding energy of the Na ions. Such effects have been observed in homovalently doped alkali and silver halide systems (31). The presence of heavier anion dopants such as $B_4O_7^{2-}$, MoO_4^{2-}, and WO_4^{2-} in the sulfate sublattice may also increase the Na ion mobility by reducing the scattering effect due to the rotating sulfate ions.

The factors discussed above, however, fail to explain the increase in the values of σ_0 with increasing dopant concentration. The high values of σ_0 above 5 mol% CO_3 and WO_4 and 10 mol% MoO_4 concentration may be attributed to the presence of either new phases or additional phases in the system, as discussed in the previous section. Evidently, the role of other structural factors, such as the rotational motion of the anion dopants and the compressibility of the lattice, has to be probed to completely understand the conductivity behavior of these systems. Because the contribution of each of these factors to the overall enhancement in σ_0 is insignificant, no further investigation was carried out in that direction.

Effect on the phase transitions. The conductivity vs $10^3/T$ plots of the doped compositions show a knee at the transition from the high-conductivity phase to the low-conductivity phase, making it difficult to pinpoint the exact phase transition temperature. This may be attributed to the partial stabilization of Na_2SO_4 (I) at lower temperatures. Bredig (32) has reported that the crystal structure(s) of the dopant is very critical in determining its ability to quench phase I at low temperatures. Their studies show that this phase can be stabilized by the addition of compounds that have low solid solubility in the low-temperature phase and, therefore, must be precipitated for transformation. Our results are in agreement with this hypothesis. The ineffectiveness of the borate ions in quenching Na_2SO_4 (I) at room temperature may be attributed to the high solubility of these ions in both the low- and high-temperature phases of Na_2SO_4.

4. CONCLUSIONS

Among the four dopants studied in the present investigation, the MoO_4 ion seems to be the most effective in increasing the conductivity of Na_2SO_4 and in stabilizing phase I at room temperature. At temperatures above 200°C, phase I is stable in most of our samples. It is well known that dopants have a high solubility in phase I. Our conclusions therefore are restricted to this phase, where the compositions studied in this work exist as a single phase.

The high conductivity of the MoO_4 doped systems is due to the following four reasons. First and most important, the presence of larger size dopants in the Na_2SO_4 lattice increases the free volume available for migration of ions. Second, the size mismatch between the anions results in an increase in the number of mobile Na ions. Third, the substituted heavier MoO_4 ions impart stability to the anion array and reduce the scattering of the mobile Na ions. Last, because the high-temperature forms of Na_2SO_4 and Na_2MoO_4 are isomorphous, an easy anion substitution is ensured in their respective lattices. The tungstate ion, with its larger size and mass, would appear to be a better candidate as a dopant for Na_2SO_4 than the molybdate ion. This is indeed the case for low (2 mol%) dopant concentration. The difference in structures of the high-temperatures phases of Na_2SO_4 and Na_2WO_4 instead ensures a low solid solubility for the WO_4 ions in the SO_4 sublattice and, consequently, reduces the effectiveness of the tungstate ion as a dopant. From the low activation energies obtained in the smaller size CO_3 and B_4O_7 ion doped systems, it is clear that the shape and orientational ordering of the dopant anions, more than their size, affect the mobility of the Na ions.

Only partial stabilization of Na_2SO_4 (I) could be achieved in the mixed anion systems at room temperature. The ability to quench phase I in the doped Na_2SO_4 system appears to depend on the crystal structure of the dopant compound.

REFERENCES

1. F. C. Kracek and R. E. Gibson, *J. Phys. Chem.* **34,** 188 (1930).
2. W. Eysel, H. H. Hofer, K. L. Keester, and Th. Hahn, *Acta Crystallogr.* **B41,** 5 (1985).
3. R. M. Murray and E. A. Secco, *Can. J. Chem.* **56,** 2616 (1978).
4. M. D. Leblanc, U. M. Gundusharma, and E. A. Secco, *Solid State Ionics* **20,** 61 (1986).
5. K. T. Jacob and D. B. Rao, *J. Electrochem. Soc.* **126,** 1842 (1979).
6. N. Imanaka, Y. Yamaguchi, S. Kuwabara, G. Y. Adachi, and J. Shiokawa, *Bull. Chem. Soc. Jpn.* **58,** 5 (1985); **23,** 15 (1987).
7. Y. Saito, K. Kobayashi, and T. Maruyama, *Thermochim. Acta* **53,** 289 (1982).
8. K. L. Keester, W. Eysel, and Th. Hahn, *Acta Crystollgr.* **A31,** S79 (1975).
9. G. Prakash and K. Shahi, *Solid State Ionics* **23,** 151 (1987).
10. E. A. Secco, *in* "Solid State Ionics—Materials and Applications" (B. V. R. Chowdari, Q. G. Liu, and L. Chen, Eds.), p. 47. World Scientific, Singapore, 1992.
11. E. A. Secco and M. G. Usha, *Solid State Ionics* **68,** 213 (1994).
12. Y. Saito, K. Kobayashi, and T. Maruyama, *Solid State Ionics* **14,** 265 (1984).
13. N. Imanaka, G. Y. Adachi, and J. Shiokawa, *Bull. Chem. Soc. Jpn.* **57,** 687 (1984).
14. N. Rao and J. Schoonman, *Solid State Ionics* **57,** 159 (1992).
15. H. Hofer, W. Eysel, and U. Von Alpen, *Matter. Res. Bull.* **13,** 135 (1978).
16. P. W. S. K. Bandaranayake and B. E. Mellander, *Solid State Ionics* **40/41,** 31 (1990); **26,** 33 (1988).
17. A. Singhvi, S. Gomathy, P. Gopalan, and A. R. Kulkarni, *J. Solid State Chem.* **138,** 183 (1998).
18. M. S. Kumari and E. A. Secco, *Can. J. Chem.* **61,** 2804 (1983).
19. M. A. K. L. Dissanayake, M. A. Careem, P. W. S. K. Bandaranayake, R. Frech, and P. A. G. Dharmasena *in* "Proceedings of the 2nd Asian Conference on Solid State Ionics—Beijing, Oct.–Nov. 1990" (B. V. R. Chowdari, Q. Liu, and L. Chen, Eds.), p. 435, World Scientific, Singapore, 1990.
20. S. Chaklanobis, K. Shahi, and R. K. Syal, *Solid State Ionics* **44,** 107 (1990).
21. A. N. Khlapova and E. S. Kovaleva, *J. Struct. Chem.* **67,** 517 (1963).
22. L. Chen, S. Yang, L.Zhao, M. Zhang and D. Li, *in* "Proceedings of the 2nd Asian Conference on Solid State Ionics—Beijing, Oct.–Nov. 1990" (B. V. R. Chowdari, Q. Liu, and L. Chen, Eds.), p. 355. World Scientific, Singapore, 1990.
23. P. H. Bottelberghs and F. R. Van Buren, *J. Solid State Chem.* **13,** 182 (1975).
24. H. E. Boeke, *Z. Anorg. Chem.* **50,** 364 (1907).
25. K. Singh and V. K. Deshpande, *Solid State Ionics* **13,** 265 (1984).
26. G. Y. Adachi, N. Inamaka, and J. Shiokawa, *Can. J. Chem.* **61,** 1557 (1983).
27. B. N. Mehrotra, Th. Hahn, H. Arnold, and W. Eysel, *Acta Crystallogr.* **A31,** S79 (1975).
28. K. B. Yatsimirski, *Izv. Akad. Nauk SSSR, Otd. Khim Nauk* 453 (1947); 398 (1948).
29. M. A. K. L. Dissanayake, M. A. Careem, P. W. S. K. Bandaranayake, R. P. Gunawardane, and C. N. Wijayasekera, *Solid State Ionics* **40/41,** 23 (1990).
30. M. A. K. L. Dissanayake and B. E. Mellander, *Solid State Ionics* **21,** 279 (1986).
31. P. Manoravi and K. Shahi, *in* "Solid State Ionics—Materials and Applications" (B. V. R. Chowdari, Q. G. Liu, and L. Chen, Eds.), p. 81. World Scientific, Singapore, 1992.
32. M. A. Bredig, *J. Phys. Chem.* **46,** 247 (1942).